[6]Dowling, D. R., "Mixing in Gas Phase Turbulent Jets," Ph.D. Thesis, Graduate Aeronautical Labs., California Inst. of Technology, Pasadena, CA, 1988.

[7]Chopra, P., and Heddle, D., "Polarization Free Measurements of Rayleigh Scattering of Lyman-α," *Journal of Applied Physics: Atomic and Molecular Physics*, Vol. 7, 1974, pp. 2421–2428.

Shear Buckling Response of Tailored Composite Plates

Sherrill B. Biggers* and Stephane S. Pageau†
Clemson University, Clemson, South Carolina 29634

Introduction

BUCKLING is frequently an important consideration in the design of aerospace and other types of structures composed of thin, plate elements. A number of authors[1–7] have addressed optimization of composite plates for buckling resistance by adjusting the design variables (fiber orientations, ply thicknesses) uniformly across the planform of the plate. However, additional aspects of tailoring can easily be exploited with composite materials to further improve buckling response. These include the variation of fiber orientation angles over the planform of the plate[8,9] and the piecewise-uniform redistribution of materials with fixed fiber orientations across the planform.[10,11] Plates tailored in these two ways have membrane and bending stiffnesses that are not uniform over the planform of the plate. These nonuniform properties can interact and can increase buckling loads with no increase in the weight of the plate. Average membrane properties are affected by the variable fiber orientation approach but they are not significantly affected by piecewise-uniform tailoring. Furthermore, with this latter approach, compressive buckling load increases up to 200% have been shown compared to uniform plates.[10,11]

This Note evaluates the piecewise-uniform approach to tailoring as a means of improving the shear buckling loads of composite plates. This design approach is referred to herein as stiffness tailoring or, more simply, as tailoring. The primary objectives are to determine the tailoring patterns and the degree of concentration of the material used to achieve the tailoring in each pattern that maximize the shear buckling load and to quantify the maximum relative improvement that can be achieved in the buckling load compared to uniform plates.

Tailoring Approach

The plate to be tailored is assumed to be flat and supported on all four sides by substructure. Furthermore, the plate is considered to be a typical element in an assembly with similar plates adjacent to each side. In an aircraft structure, for example, the plate could represent a portion of the wing skin or a large-radius fuselage skin supported on its four sides by ribs, frames, spars, or stringers. The tailoring concepts investigated include diagonal patterns which are doubly symmetric with respect to the in-plane vertical and horizontal directions so that the sign of the shear load is inconsequential. In addition, only those concepts which permit all fibers to be continuous across the plate and between adjacent plates are considered.

Figure 1 illustrates two typical acceptable tailoring patterns and two unacceptable ones. In this figure, the darker areas are regions to which material has been relocated and are therefore thicker and stiffer than the lighter areas. Diagonal bands represent areas to which +45 or −45 deg material has been redistributed. With these restrictions on the tailoring geometry, all laminae are continuous in their fiber directions and no stress concentrations associated with fiber drop-off in the fiber direction are present. Local stress concentrations due to fiber joggles will, however, be present. These local stress concentrations are the subject of ongoing work but are not considered in this study. Fiber joggles could be minimized or eliminated if lightweight core material were added in the thinner regions to create a tailored sandwich plate. Results for tailored sandwich concepts are to be presented elsewhere. Simple schematics of possible geometries are shown in Fig. 2. Notice that these configurations have varying degrees of fiber joggles and have one or two flat external surfaces. All of the results reported herein correspond to concepts that have a flat midplane and laminates that are symmetric through the thickness relative to the midplane.

Finite Element Model

Buckling loads are computed for uniform and tailored plates using the ABAQUS finite element code.[12] Pure in-plane shear deformation is applied to the plate edges which, for compatibility with adjacent plates in an actual structure, are required to remain straight. Both positive and negative eigenvalues, corresponding to positive and negative applied shear loading, are computed. The eigenvalue with the lowest absolute value is taken as the critical buckling load. The elements chosen for the analysis are the eight-node quadrilateral anisotropic shear deformable (first-order shear theory) shell elements denoted S8R5 in the ABAQUS code. In some cases, the quadrilateral elements are degenerated to triangular elements. The relatively low transverse shear stiffness of composite materials can significantly affect the buckling loads of composite plates. This effect of transverse shear deformation becomes increasingly negative in regions where the plate thickness is increased due to tailoring. As a result, transverse shear deformation has a greater influence on the buckling loads of tailored plates than uniform plates[10] and must be included in the evaluation so that the benefits of tailoring are not overestimated. Model refinement needed to yield buckling loads within about 1% of converged values was determined for selected highly tailored cases. This level of refinement was used in generating the results shown herein.

Material Properties

Material properties representative of an intermediate modulus fiber, toughened resin composite (IM7/8551-7) are used. The following relative properties are taken from Dow[13]: $E_{11}/E_{22} = 13.90$, $G_{12}/E_{22} = 0.48$, and $\nu_{12} = 0.33$

Values for G_{13} and ν_{13} are assumed equal to G_{12} and ν_{12}, respectively. A value for G_{23} was calculated from micromechanics using the fiber volume fraction from Dow[13] and manufacturer's data for the shear stiffnesses of the matrix and the fiber. The resulting relative transverse shear modulus is $G_{23}/E_{22} = 0.305$.

Parametric Study

The baseline plate used for comparison in this study is a uniform, quasi-isotropic, 16-ply laminate with layup $[\pm 45/0/90]_{2s}$ and a width-to-thickness ratio of 100. Based on results for compressive buckling,[10] the effect of transverse shear deformations for this thin plate should be negligible for the uniform plate and on the order of 3–5% for the tailored plates. However, these effects are included in the reported results regardless of their magnitude. The primary design variables are the basic pattern of the tailoring and the degree to which material is redistributed in these patterns. The latter is quantified by a width ratio $\bar{b}$ defined as the total width b_1 of the stiffened regions (the darkened regions in Fig. 1) measured along a ±45-deg line divided by the total width $\sqrt{2}\,b$ along the diagonal.

The shear buckling loads for the tailored plates are reported as normalized buckling loads $\bar{N}_{xy}$ where the buckling load of the uniform baseline plate is used as the normalizing factor. Because of the variation of stiffness across the tailored plates and the imposition of uniform shear deformation, the shear loads on the edges of

Received Feb. 11, 1993; presented as Paper 93-1408 at the AIAA/ASME/ASCE/AHS/ASC 34th Structures, Structural Dynamics, and Materials Conference, La Jolla, CA, April 19–21, 1993; revision received Aug. 20, 1993; accepted for publication Sept. 2, 1993.

*Associate Professor, Department of Mechanical Engineering. Senior Member AIAA.

†Research Assistant, Department of Mechanical Engineering.

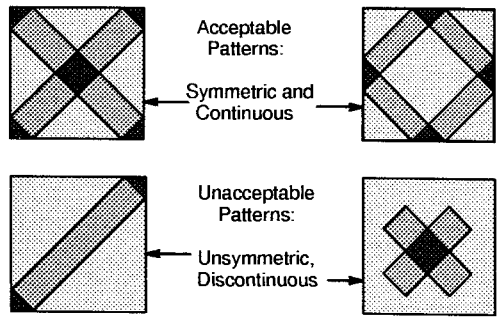

Fig. 1 Typical acceptable and unacceptable tailoring patterns for shear buckling.

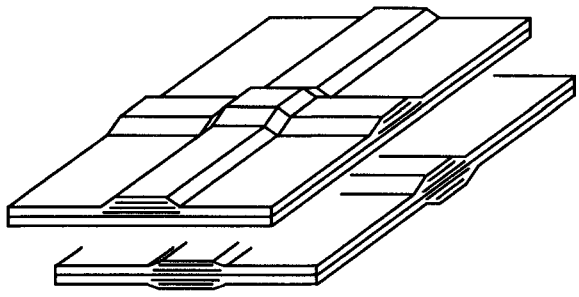

Fig. 2 Sample fabrication options.

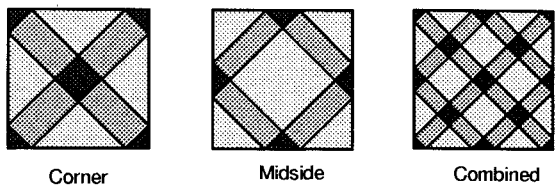

Fig. 3 Diagonal tailoring patterns.

the plates are nonuniform. The $\bar{N}_{xy}$ values are average shear buckling loads per unit length along the edges of the plate. This nonuniformity of shear edge loads brings into question the point made in the Introduction that stiffness tailoring does not appreciably affect the average membrane stiffnesses of the plate. Results are presented for the normalized average shear stiffness $\bar{A}_{66}$ as a function of $\bar{b}$. The membrane shear stiffness of the uniform baseline plate is used as the normalizing factor in computing $\bar{A}_{66}$.

Tailoring Concepts

Each plate is assumed to have a flat midplane and to have stacking sequences that are symmetric about the midplane at all locations. The effect of tailoring with one side flat, rather than with the midplane flat, was shown to be a small increase on compressive buckling loads.[10] A similar small increase is expected for shear buckling.

Three diagonal tailoring patterns are evaluated. Each pattern satisfies the symmetry and continuity requirements discussed earlier. The patterns will be referred to as the corner, midside, and combined patterns and are shown schematically in Fig. 3. In each case, only the ±45-deg fibers are redistributed to create the tailored plate. All of the ±45-deg material is used in the tailoring, thus creating layups of $[0/90]_{2s}$, $[(+45 \text{ or } -45)_n/0/90]_{2s}$, and $[\pm 45_n/0/90]_{2s}$ in the thinnest, stiffened, and crossover regions, respectively. The value of n is the inverse of the width ratio $\bar{b}$.

Normalized shear buckling loads $\bar{N}_{xy}$ for simply supported plates are shown in Fig. 4 as a function of the width ratio $\bar{b}$. Increasing the width ratio corresponds to increasing the thicknesses of the stiffened and crossover regions. For example, in the highly tailored case with the width ratio $\bar{b} = 0.25$ ($n = 4$), the maximum thickness at the crossover locations becomes 2.5 times the thickness of the baseline plate. The stiffened region between crossovers is 1.5 times as thick as the baseline plate. The thinnest region is half as thick as the baseline plate. While very large improvements in buckling load can be obtained for smaller width ratios, these thickness variations are taken as upper limits in this study and no results are shown for $\bar{b} < 0.25$. In some cases, higher limits on $\bar{b}$ may be imposed for practical reasons. Such limits are, of course, application dependent.

Examination of these data indicates that tailoring with the corner or midside patterns actually decreases the shear buckling load for all but the smallest values of $\bar{b}$. However, the combined pattern produces increases in the buckling load for all width ratios, with a maximum increase of about 75% above the uniform plate. The fact that the combined pattern exceeds the performance of both the corner and midside patterns as well as that of the uniform plate is counter-intuitive and suggests that a complex interaction of geometric, stiffness, and load distribution effects is occurring. These results are distinctly different from those previously shown for pure compressive buckling.[10] There, all values of $\bar{b}$ were shown to correspond to improvements in buckling load and true optimum values of $\bar{b}$ were shown to exist in the range of $\bar{b} = 0.25$ to 0.40. Corresponding peak improvements in compressive buckling loads were shown to exceed 100% to 200% depending on the baseline laminate. The current results show that maximum buckling loads correspond to the minimum permissible width ratios.

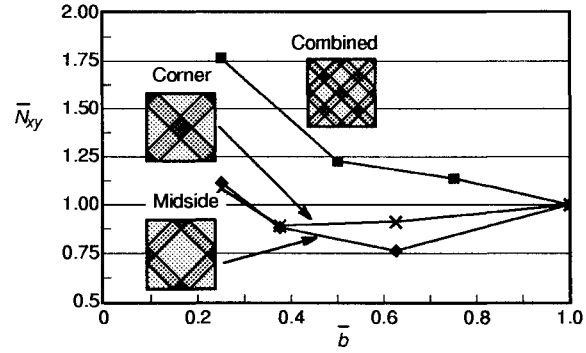

Fig. 4 Normalized shear buckling loads for simply supported, square plates.

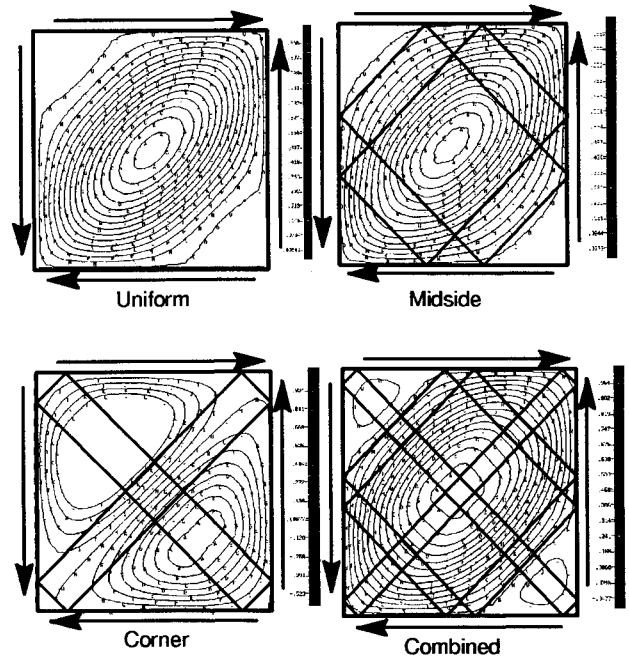

Fig. 5 Shear buckling mode shapes.

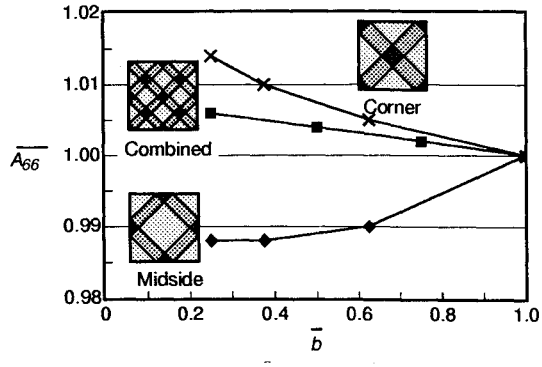

Fig. 6 Normalized average membrane shear stiffness.

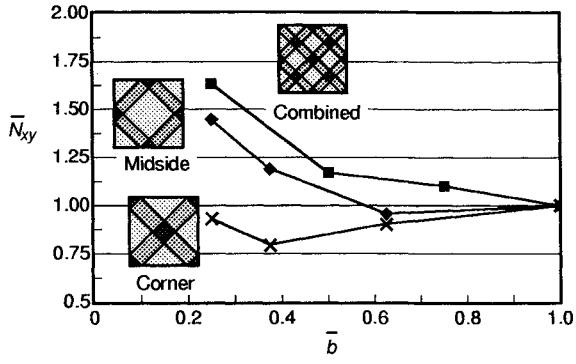

Fig. 7 Normalized shear buckling loads for clamped plates.

These results also show that stiffness tailoring is more effective for compressive loading than for shear loading. However, a 75% increase in shear buckling load is significant and tailoring could be used to advantage with the combined pattern.

Contour plots of the transverse deflections associated with the critical buckling modes for the three diagonal patterns are shown in Fig. 5. These modes correspond to plates with $\bar{b} = 0.25$. The outlines of tailoring patterns are overlaid on the contour plots so that the relationship of stiffened regions to the deformations may be easily seen.

The statement made earlier that the stiffness tailoring concepts investigated do not substantially change the average membrane shear stiffness of the plate is substantiated by the data in Fig. 6. Here the normalized average membrane shear stiffness $\bar{A}_{66}$ is shown as a function of $\bar{b}$. Only about a 1% change in the membrane shear stiffness is produced with any of the tailoring patterns.

Results similar to those shown in Fig. 4 are presented in Fig. 7 for square plates that are clamped on all sides. The normalizing buckling load is the buckling load for the baseline plate with all sides clamped. The trends are very similar to those observed from the data in Fig. 4. The combined pattern is again the superior one with the maximum improvement of the buckling load at about 65%.

The effectiveness of stiffness tailoring in increasing the shear buckling load of rectangular plates is indicated by the data presented in Fig. 8. Here the plate length is twice the plate width, all sides are simply supported, and the corner and combined patterns are evaluated. The buckling load for a uniform plate with aspect ratio 2:1 is used as the normalizing factor and the plate width is used in the definition of $\bar{b}$. Although the buckling modes and the buckling loads are different from those of the square plates, the normalized buckling loads vary with $\bar{b}$ in a way similar to those shown in Fig. 4 for square, simply supported plates. The combined pattern is again the better pattern, producing about an 85% improvement in the buckling load compared to the baseline rectangular plate. Although longer plates have not been investigated, these results suggest that the effect of tailoring on the normalized buckling loads of longer plates would be quite similar to the effects shown for square and the 2:1 rectangular plate.

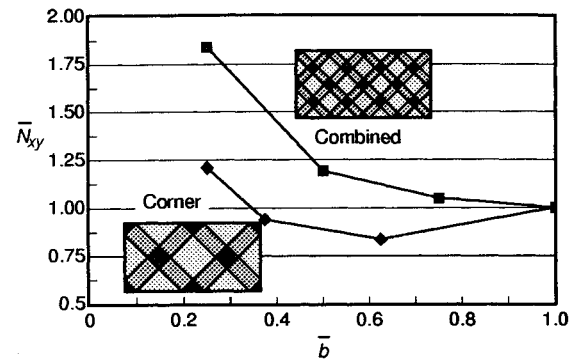

Fig. 8 Normalized shear buckling loads for simply supported, rectangular plates.

Summary and Conclusions

A simple, piecewise-uniform stiffness tailoring concept has been shown to be an effective way to increase the buckling load in composite plates loaded in shear with no sacrifice in weight and no substantial change in average in-plane stiffness. Some specific conclusions reached in this research follow:

1) A redistribution of ±45-deg material in a diagonal pattern can produce increases in buckling loads in square plates of up to 75% compared with uniform plates. The best diagonal tailoring pattern is a combination of a corner-to-corner and a midside-to-midside pattern. Buckling loads for this combined pattern do not lie between those for the corner and midside patterns but, instead, exceed those of either pattern.

2) Tailoring clamped-edge plates provides a slightly lower increase in buckling load (up to 65%) than simply supported plates.

3) Rectangular plates (2:1 aspect ratio) can be tailored with a slightly higher degree of effectiveness (up to 85% improvement) than square plates.

4) The maximum increase in shear buckling load occurs for the smallest permissible width ratios $\bar{b}$. The benefit of tailoring for shear buckling will, therefore, be a function of this limit as set by practical considerations associated with each application.

5) Comparison of the data reported herein for shear loading to that reported previously for compressive loading indicates that tailoring is more effective in increasing compressive buckling loads than shear buckling loads.

Acknowledgment

This research was supported by NASA Langley Research Center under Grant No. NAG-1-1141 to Clemson University.

References

[1]Chao, C. C., Koh, S. L., and Sun, C. T., "Optimization of Buckling and Yield Strengths of Laminated Composites," *AIAA Journal*, Vol. 13, No. 9, 1975, pp. 1131, 1132.

[2]Hirano, Y., "Optimum Design of Laminated Plates under Axial Compression," *AIAA Journal*, Vol. 17, No. 9, 1979, pp. 1017–1019.

[3]Hirano, Y., "Optimum Design of Laminated Plates under Shear," *Journal of Composite Materials*, Vol. 13, Oct. 1979, pp. 329–334.

[4]Stroud, W. J., and Anderson, M. S., "PASCO: Structural Panel Analysis and Sizing Code, Capability and Analytical Foundations," NASA TM-80181, Jan. 1980.

[5]Shin, Y. S., Haftka, R. T., Watson, L. T., and Plaut, R. A., "Design of Laminated Plates for Maximum Buckling Load," *Journal of Composite Materials*, Vol. 23, No. 4, 1989, pp. 348–369.

[6]Nagendra, S., Haftka, R. T., and Gurdal, Z., "Stacking Sequence Optimization of Simply Supported Laminates with Stability and Strain Constraints," *AIAA Journal*, Vol. 30, No. 8, 1992, pp. 2132–2137.

[7]Chai, G. B., Ooi, K. T., and Khong, P. W., "Buckling Strength Optimization of Laminated Composite Plates," *Computers and Structures*, Vol. 46, No. 1, 1993, pp. 77–82.

[8]Olmedo, R.A., and Gurdal, Z., "In-Plane and Buckling Response of Composite Panels with Curvilinear Fibers," Center for Composite Materials and Structures, Virginia Polytechnic Inst. and State Univ., CCMS-92-28, Blacksburg, VA, Sept. 1992.

[9]Gurdal, Z., and Olmedo, R., "In-Plane Response of Laminates with Spatially Varying Fiber Orientations: 'Variable Stiffness Panel Concept'," *AIAA Journal*, Vol. 31, No. 4, 1993, pp. 751–758.

[10]Biggers, S. B., and Srinivasan, S., "Compression Buckling Response of Tailored Rectangular Composite Plates," *AIAA Journal*, Vol. 31, No. 3, 1993, pp. 590–596.

[11]Biggers, S. B., and Srinivasan, S., "Improved Compression Buckling for Rectangular Composite Plates by Stiffness Tailoring," *Enhancing Analysis Techniques for Composite Materials*, NDE Vol. 10, ASME, New York, 1991, pp. 187–195.

[12]HKS (Hibbitt, Karlsson, and Sorensen), Inc., *ABAQUS Theory and User's Manuals, Version 4.8*, HKS, Pawtucket, RI, 1989, pp. 2.2.7-1, 3.4.3-1–3.4.3-6.

[13]Dow, M. B., and Smith, D. L., "Properties of Two Composite Materials Made of Toughened Epoxy Resin and High-Strain Graphite Fiber," NASA TP-2826, 1988.

Damage Detection in Framed Structures

Izhak Sheinman*
Technion—Israel Institute of Technology, Haifa, Israel

Introduction

INTRODUCTION of advanced new materials and "smart" structures is strongly conditional on ability to assure their safety. In the course of their service life, load-carrying structural systems undergo damage which should be monitored with respect to occurrence, location, and extent. The new nondestructive test procedures developed following the rapid advances in testing equipment and techniques are mostly based on modal analysis and entail a relatively large volume of measurements which limits their suitability for practical application. Hence the need for a solution involving minimal measurements.

Systematic methods put forward in recent years and combining test data with analysis may be used for damage detection as well. Some of these (for example, Refs. 1 and 2) propose optimization procedures for correcting the stiffness and mass matrix on the basis of measured modes, irrespective of the physical meaning of the connectivity. Others (like Refs. 3 and 4) offer mathematical procedures which preserve the original connectivity and consequently reduce the required volume of measurements. A closed-form algorithm for precise detection, using test data and likewise preserving the connectivity, is given in Ref. 5. This algorithm identifies the damaged degrees of freedom (DOF) and then solves a set of equations to yield the damaged stiffness coefficients. Its drawback is that even a small number of damaged DOFs may result in a large number of damaged stiffness coefficients with the corresponding excessive measurement volume. Accordingly, this Note presents a new algorithm which preserves the ratio of stiffness coefficients besides the connectivity, and thus significantly reduces the needed measurements. The algorithm identifies the damaged members through very few measured modes, and is suitable for large structures with thousands of degrees of freedom. It is suitable for framed structures in which the DOFs are disturbed by the damage to the members rather than by that to the joints, so that the algorithm should refer to the affected members instead of the stiffness coefficients.

The algorithm is developed for the general case of damage in both the stiffness and mass matrices, in which case static measurements are for the former, and then dynamic ones for the latter. Where only one matrix is damaged, either static or dynamic measurements are called for in the case of the stiffness matrix, and only dynamic ones in that of the mass matrix. The present algorithm is confined for framed structures (truss and beam members), and does not address the issue of noise, as it is based on real test data (which are assumed to be accurate).

Received May 4, 1993; revision received Sept. 29, 1993; accepted for publication Sept. 30, 1993.

*Professor, Faculty of Civil Engineering.

Analytical Formulation

The procedure is based on the following equation:

$$[\Delta R]\{\phi_{im}\} = \{y_{di}\} \tag{1}$$

where

$$[\Delta R] = [\Delta K] - \omega_{im}^2 [\Delta M]$$
$$\{y_{di}\} = [\omega_{im}^2 M_o - K_o]\{\phi_{im}\} \tag{2}$$

K_o and M_o are the stiffness and mass matrices of the undamaged system; ΔK and ΔM are the respective amounts of damage to the matrices; ω_{im} and ϕ_{im} are the measured ith frequency and ith eigenmode; and y_{di} is the force residue at all DOFs created by the damage.

The location of the damage is determined directly by identifying the DOFs (j) whose force residue $y_{di}(j)$ is not zero. This can be done through a single measured mode, provided the latter is affected by the DOF in question. Since ΔR contains the unknown stiffness and mass coefficients, it is desirable to rewrite Eq. (1) as

$$[C]\{\bar{\Delta R}\} = \{Z_{di}\} \tag{3}$$

where $\bar{\Delta R}$ is the unknown vector containing only the terms of ΔRej appearing in the jth equation for which $y_{di}(j) \neq 0$. Z_{di} is the vector consisting of the nonzero terms of y_{di} and $[C]$ the coefficient matrix consisting of the measured eigenmode parameters.

As the connectivity is assumed to be preserved, $[C]$ can be decomposed into uncoupled regions (of order N, N being the number of unknown stiffness coefficients for the current damaged zone) which are solvable separately (see Ref. 5), with the attendant significant saving in computer time. It should be noted that Eq. (3) yields the exact $\bar{\Delta R}$ vector provided the measured modes are exact. However, the number of measured modes which are needed for solving Eq. (3) is increasing with the number of DOFs of the ends of the damage zone. For example, for a plane beam element it may require up to four measured modes and for a space beam element up to 12 measured modes (irrespective of the number of elements in the damaged zone).

In the case of a damaged stiffness matrix, a procedure based on preserving the ratio of stiffness coefficients (meaning the effect of damage is the same on all terms which are connected) makes for significant reductions of the number of measured modes. Preservation of the connectivity, irrespective of where the modes are measured, yields the exact damage vector $\bar{\Delta R}$. By contrast, preservation of the ratio of stiffness coefficients implies that the damage is uniquely distributed in between the measured damaged DOFs. Hence, for the ratio to be preserved the damaged zone should be exactly located, the modes are then measured at its ends and the damage of the stiffness matrix, at each affected zone, is calculated from

$$[C]_{N*N}\{\bar{\Delta K}\}_{N*1} = \{Z_{di}\}_{N*1} \tag{4}$$

(in the case where the mass matrix is also damaged, Eq. (4) is derived from static measurements).

Since the coefficient ratios of the stiffness matrix are preserved, $\{\bar{\Delta K}\}$ can be expressed in terms of the damaged properties of the members. In framed structures, these are EA, GJ, EI_1, and EI_2, where E is the modulus of elasticity, G is the shear modulus, A is the cross-sectional area, and J, I_1, I_2 are the moments of inertia in the axial and transverse directions. For general case of a different damage amount to each property, the local stiffness matrix of the member (which comprised the submatrix for the jth end in the member stiffness matrix) can be written as

$$[K]_m = (EA)_m[K_1]_m + (GJ)_m[K_2]_m + (EI_1)_m[K_3]_m + (EI_2)_m[K_4]_m \tag{5}$$